Surface & Coatings Technology 237 (2013) 440–444

Contents lists available at ScienceDirect

Surface & Coatings Technology

journal homepage: www.elsevier.com/locate/surfcoat

Dual frequency ICP discharges: Effect of pressure and gas ratio on EEPF and discharge parameters

Anurag Mishra [a], Geun Young Yeom [a,b,*]

[a] Department of Advanced Materials Science and Engineering, Sungkyunkwan University, Suwon, Gyeonggi-do, 440-746, South Korea
[b] SKKU Advanced Institute of Nanotechnology (SAINT), Sungkyunkwan University, Suwon, Gyeonggi-do 440-746, South Korea

ARTICLE INFO

Available online 12 October 2013

Keywords:
Dual frequency ICP discharges
Electron energy distribution
Plasma density
Plasma potential
Pressure dependent effects
Time-resolved plasma potential

ABSTRACT

Using a radio frequency (rf) compensated Langmuir probe, the effects of operating parameters such as gas pressure and gas ratio on electron energy probability functions (EEPFs) and discharge parameters are investigated in Ar/CF_4 discharges produced by a dual frequency/dual antenna large area (450 mm) inductively coupled plasma (ICP) source. It is observed that increasing pressure reduces the energy spread of EEPFs, due to increasing electron energy loss via collisions, from 20 eV at 1 mTorr to 13 eV at 25 mTorr. At a constant rf power, plasma density (n_e) increases linearly with pressure between 1 and 10 mTorr and then (>10 mTorr) decreases. The same trend has also been observed for electron temperature. It has also been found that increasing Ar gas proportion in the Ar/CF_4 mixture significantly increases the plasma density (n_e), however, the influence on plasma temperature and plasma potential was marginal.

1. Introduction

The plasma processing is a key step in the microelectronic industry for the fabrication of various semiconductor devices [1–3]. To keep pace with the 'Moore's law' and to fulfill the quest for fabricating the smallest possible microelectronics devices, the semiconductor industry presently is looking forward to moving for fabrication of electronic devices at the critical dimension of a few tens of nano-meter level. The fabrication at the nanometer level increases the manufacturing cost, therefore, it is necessary to adopt processing at a large area wafer size in order to improve productivity and optimize the fabrication cost. According to a technology trend forecast, the wafer size will be 450 mm in diameter within a few years [4,5]. However, the transition towards processing at large wafer areas poses several technological issues. One of them is decoupling ion energy and reactants flux density so that these two parameters could be controlled separately. Second one is the high uniformity over the large wafer surface area.

In order to control the plasma density (n_e) and ion energy distribution (IED) over the substrate separately, the application of two different frequencies, high and low frequencies, on top and bottom electrode respectively has been proposed [6–8]. This modified technique is known as dual frequency capacitively coupled plasma (DF-CCP) discharges. In this technique, a higher frequency (ranging from few tens MHz to few hundreds of MHz) is applied on the top electrode and lower frequency (typically 2 MHz, ranging from a few to 10 MHz) on the bottom electrode or both frequencies on either electrode. In this technique, plasma density is controlled by the high frequency (f_h) whereas the ion bombarding energy by the low frequency (f_l). The high frequency (f_h) determines plasma density as $n_e \propto f^2 V_{rf}$ and the low frequency determines the ion bombarding energy as IED $\propto (|V_h + V_l|)$ and $V_h \ll V_l$, where V_{rf} is rf voltage, V_f is the V_{rf} for the high frequency, and V_l is the V_{rf} for the low frequency. Therefore, for the separate control over plasma density and ion bombarding energy, ($f_h^2|V_h| \gg f_l^2|V_l|$) should be satisfied. That is the reason, decoupling the two sources often requires that the sources need to be operated at significantly different frequencies ($f_h \gg f_l$), for an example, f_l at 10 MHz and f_h at 100 MHz. However, an investigation of space and phase resolved optical emission spectroscopic in dual frequency-CCP discharges revealed a strong coupling of low and high frequencies in the emission profiles [9]. The control of plasma density by the high frequency was, therefore, also influenced by the low frequency.

In addition, increasing the high frequency of the dual frequency-CCP introduces electromagnetic wave effects, which are detrimental to the uniformity of the plasma [10–13]. These effects include constructive and destructive interference and skin effects. The voltage applied to the rear of the electrode propagates around the edges of the electrode to enter the plasma. The electric field, caused by applied voltage, does not significantly penetrate into the conductive bulk plasma and is wave-guided in the sheath at the surface of the electrode. At a sufficiently low frequency (long wavelength λ), the electric field is uniformly distributed within the sheath, along to the electrode. For a sufficiently high frequency (short wavelength), the interference

* Corresponding author at: Department of Advanced Materials Science and Engineering, Sungkyunkwan University, Suwon, Gyeonggi-do, 440-746, South Korea.
E-mail address: gyyeom@skku.edu (G.Y. Yeom).

0257-8972/$ – see front matter © 2013 Elsevier B.V. All rights reserved.
http://dx.doi.org/10.1016/j.surfcoat.2013.09.063

between counter-propagating waves from opposite sides of the electrode causes nodes and antinodes of the electric field within the sheath. This results in a non-uniform discharge distribution over the substrate area. Due to the low power coupling characteristics of the electrostatic coupling, these CCP discharges cannot be operated at low pressures (<10 mTorr), a necessary requirement for the anisotropic etching.

The ability of being operated at low pressures due to strong power coupling through electromagnetic field, a high density plasma, easier plasma uniformity control, and the separation of discharge production and ion acceleration mechanism of the inductively coupled plasma (ICP) sources turned the research direction towards developing and investigating the ICP sources for some of the applications of large area microelectronic device fabrication. Recently, a novel approach, based on utilization of a dual frequency and a power splitting mechanism, has been proposed and demonstrated a discharge uniformity up to ~96% over the substrate of 450 mm in diameter [14]. Langmuir probe and mass-spectrometric measurements revealed that plasma parameters i.e. electron and ion energy distribution functions can be efficiently modulated by varying the power ratios of low and high frequencies [15,16].

Operating pressure is one of the important parameters that determine the processes (ionization mechanism, electron energy, etc.) occurring in the discharge and thus influence etch characteristics or properties of deposited thin film. Therefore, the investigation of pressure effect on the discharge parameters provides a wealth of information about physical processes occurring within the discharge volume. The present study has been carried out to investigate the effect of operating pressures, gas ratios of Ar/CF_4, and rf powers on the discharge parameters for a large area dual frequency ICP source.

The plasma parameters such as electron energy distribution, plasma density, electron temperature, and plasma potential have been measured by using an ESPion Langmuir probe system (Hiden Analytical Ltd., United Kingdom). An rf compensation unit with a broad band resonance filter (2 to 60 MHz) has been used together with the Langmuir probe to prevent the rf incursion on the probe sheath potential and to filter out rf components that distort current–voltage (I–V) characteristics [17–19]. The probe tip, located at centre and 30 mm above the substrate, is made of tungsten wire, 0.15 mm in diameter and 10 mm in length. To minimize the random noise in the I–V characteristics, a single I–V characteristics scan has been acquired by sampling a single point 10 times and then 10 scans have been averaged to get one final scan. I–V characteristics acquired by the probe system have been analyzed by a purpose built MATLAB code. The Druyvesteyn approach has been adopted in deriving the EEPFs from the I–V characteristics. In that approach, the second derivative of electron probe current I''_e with respect to the probe potential in reference to the plasma potential ($V_p - V_b$, where V_p is the plasma potential and V_b is the probe potential) is proportional to the EEPF and it has been obtained by numerically double differentiating the I–V characteristics as follows:

$$g(\varepsilon) = \frac{2m}{e^2 A}\left(\frac{2\varepsilon}{m}\right)^{\frac{1}{2}} I''_e(\varepsilon) \tag{1}$$

And the effective temperature T_{eff} has been estimated by using the following relation [15]

$$\langle\varepsilon\rangle = \frac{1}{n_e}\int_0^\infty g_e(\varepsilon)d\varepsilon \tag{2}$$

$$T_{eff} = \frac{2}{3}\langle\varepsilon\rangle \tag{3}$$

where ε, m, e, and A are the electron energy, electron mass, electron charge, and the area of the probe tip. The Savitzky–Golay filter, a polynomial order of 3 and the data frame length (N_L) of 51, is used to smooth the I–V curves. To eliminate the distortion produced by the Savitzky–Golay filter at the end data points, $(N_L + 1)/2$ data points at both data ends are made zero [20].

2. Experimental set-up

The schematic of the experimental set-up and the acquisition circuit is shown in Fig. 1. The measurements have been carried out in a cylindrical anodized aluminum chamber, 650 mm in diameter and 400 mm in length. The chamber walls were grounded. The base pressure of $\leq 1\times10^{-5}$ Torr has routinely been achieved using a turbo-molecular pump backed by a dry pump with the pumping speed of 1867 l/min (ADP 122 P from Alcatel). The pressure inside the chamber has been controlled by using a mass flow controller (2900 series, Tylan) together with an adaptive pressure controller (PM-7, VAT) for the gate valve control. The argon gas in the chamber was evenly distributed by using a multi-hole shower ring located near to the circumference of the chamber.

The discharge has been produced by using an external type dual antenna-dual frequency ICP source, which was separated from the main processing chamber by a dielectric window [14]. The inner (13 turns) and outer coils (3 turns) have been energized by 2 MHz rf (NOVA - 50 A, ENI) power supply and 13.56 MHz rf power supply (CX-5000S, COMDEL), respectively, via respective automatic matching networks. The operating pressure has been varied from 1 to 25 mTorr. The applied rf power was varied from 100 to 800 W for 2 and 13.56 MHz, both.

3. Results and discussion

The EEPFs have been plotted in a semilog plot to display them over a wide dynamic range. The EEPFs measured with the dual frequency ICP at center of substrate ($r = 00$ and $z = 70$ mm) at 1 mTorr of operating pressure and two gas ratios of Ar/CF_4 (100/400 and 200/300 sccm) are shown in Fig. 2. The rf powers to each ICP coil of 2 MHz and 13.56 MHz were kept same at 1000 W. At this pressure level, the discharge operates close to ion mean free path (Tonk–Langmuir) regime, where ion mean free path (λ_i) is comparable to characteristic extension of plasma (L), whereas electron mean free path (λ_e) is very

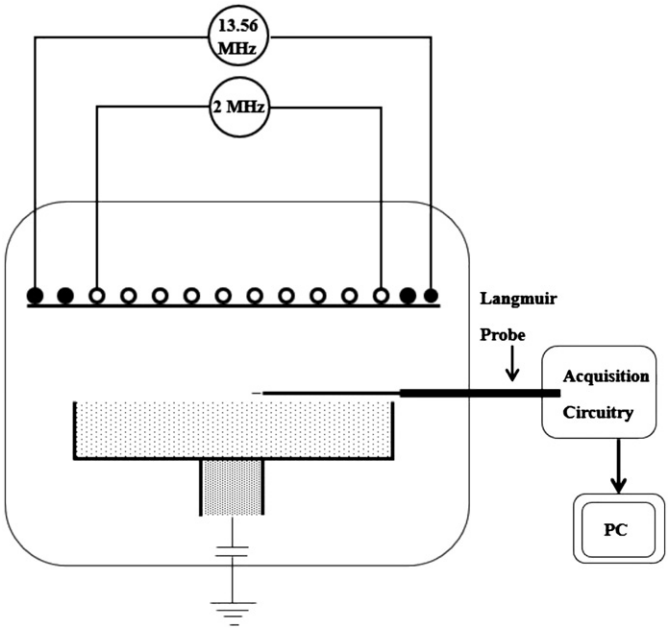

Fig. 1. Schematic diagram (not to scale) of the dual frequency-ICP discharge chamber and acquisition circuitry (Langmuir probe) system used in this study.

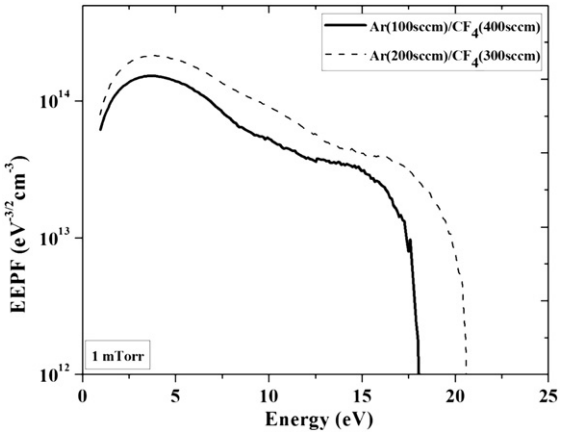

Fig. 2. EEPFs at the pressure of 1 mTorr for the rf powers of 1000 W/1000 W ($P_{2MHz}/P_{13.56\ MHz}$) and at the two Ar/CF_4 gas flow ratios of 100 sccm/400 sccm and 200 sccm/300 sccm.

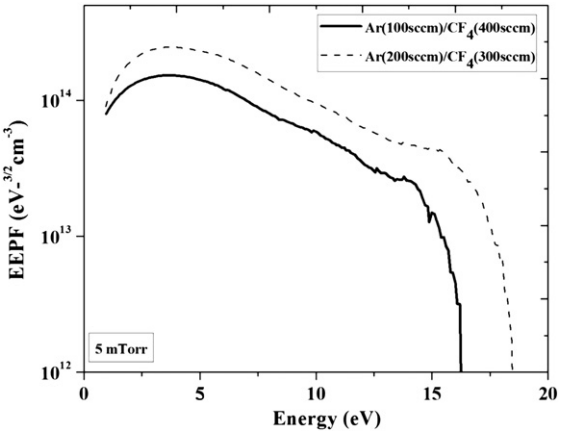

Fig. 4. EEPFs at the pressure of 5 mTorr for the rf powers of 1000 W/1000 W ($P_{2MHz}/P_{13.56\ MHz}$) and at the two Ar/CF_4 gas flow ratios of 100 sccm/400 sccm and 200 sccm/300 sccm.

large ($\lambda_i \sim L, \lambda_e \gg L$) [21]. In this regime, plasma loss to the chamber walls is controlled by ion inertia. At this pressure range, direct impact ionization is the dominant process. The first change in EEPF slope occurs close to excitation energy (10.9 V) of CF_4 and second change in slope at ionization energy (14.4 V) of CF_4 [22,23]. As the ratio of argon gas increases (Ar/CF_4: 100/400 to 200/300 sccm), the plasma density increases and, therefore, the EEPF in the elastic energy range ($\varepsilon < \varepsilon^*$) evolves into a Maxwellian distribution due to the enhancement in the electron–electron collisions leading to the equalization of the distribution temperature $T_{ed} = -[\mathrm{d} \ln f(\varepsilon)/\mathrm{d}\varepsilon]^{-1}$ [21] of low and middle energy electron groups at Ar/CF_4: 200/300 sccm. The high energy tail of EEPF extends with increasing the argon gas ratio. The CF_4 proportion was decreased with increasing argon gas ratio at a fixed total gas flow rate. Therefore, the dissociation events of CF_4 are decreased and, which resulted in the reduced electron energy loss and extended the high energy tail of the EEPF.

The EEPFs sampled at 2 mTorr are shown in Fig. 3 and have a similar EEPF shape as those in Fig. 2. However, it can be seen clearly that the three-temperature structure of the EEPFs at the pressure of 2 mTorr is less pronounced than that for 1 mTorr. Plasma density increases with increasing pressure and it increases electron–electron collisions and maxwellenizes the EEPFs at the low energy region. It makes three-temperature structure of the EEPFs less pronounced at this pressure. This trend of mazwellenizing of EEPFs increases with increasing argon gas ratio (see Fig. 3 at Ar/CF_4: 200/300 sccm).

Fig. 4 shows the EEPFs at 5 mTorr. The EEPFs evolve to a two-temperature structure (Druyvesteyn type) and very close to the Maxwellian in elastic energy range ($\varepsilon < \varepsilon^*$, where ε^* is the first excitation energy of argon and equals to 11.55 V). This observation is common to high density plasmas [21]. At level of high density, the electron–electron collision frequency (ν_{ee}) increases (as $\nu_{ee} \propto n\, \varepsilon^{3/2}$) and tends to equalize the electron temperatures, and thus maxwellenizes the EEPFs. From the Fig. 4, it is also clear that the electron temperature (which is proportional to the inverse slope of the EEPF) is marginally dependent of the gas ratio, used in this study.

The EEPFs acquired at 25 mTorr are shown in Fig. 5. At this pressure, the discharge is mainly collisional dominated and is very close to Maxwellian. The elastic energy range up to where the EEPF remains as Maxwellian reduces with increasing pressure and at the pressure of 25 mTorr, it is ~8.5 V. The electron temperature at this pressure is independent of the gas ratio. The energy spread has a tendency to shift towards low energy side with increasing pressure (see Fig. 6). It is due to the energy loss of high energy electrons via electron–neutrals collisions and thus increases the ionization.

To investigate the effect of the rf powers ratio on the both frequencies ($P_{2MHz}/P_{13.56MHz}$) on EEPFs at a fixed total power, a series of experiments has been carried out. The total power ($P_{2MHz} + P_{13.56MHz}$) is fixed at three values of 2250, 2000 and 1750 W. The pressure is 1 mTorr. The EEPFs have been plotted in normal linear plot to illustrate the effect power ratio on plasma density more clearly. The measurements shown in Fig. 7 illustrate

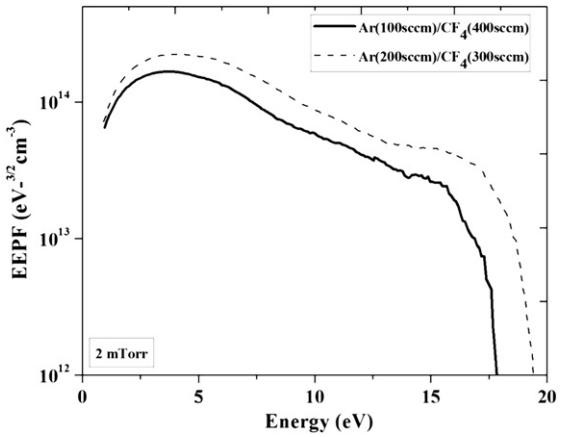

Fig. 3. EEPFs at the pressure of 2 mTorr for the rf powers of 1000 W/1000 W ($P_{2MHz}/P_{13.56\ MHz}$) and at the two Ar/CF_4 gas flow ratios of 100 sccm/400 sccm and 200 sccm/300 sccm.

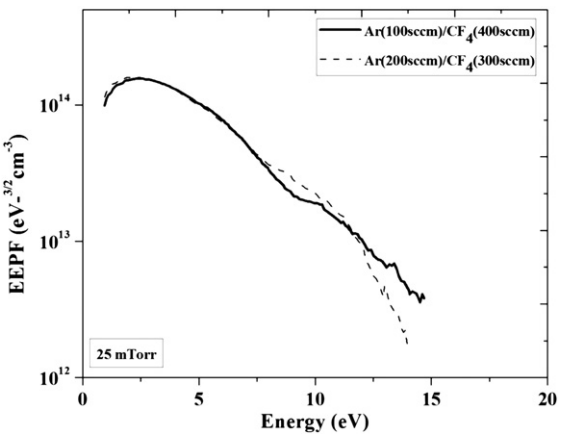

Fig. 5. EEPFs at the pressure of 25 mTorr for the rf powers of 1000 W/1000 W ($P_{2MHz}/P_{13.56\ MHz}$) and at the two Ar/CF_4 gas flow ratios of 100 sccm/400 sccm and 200 sccm/300 sccm.

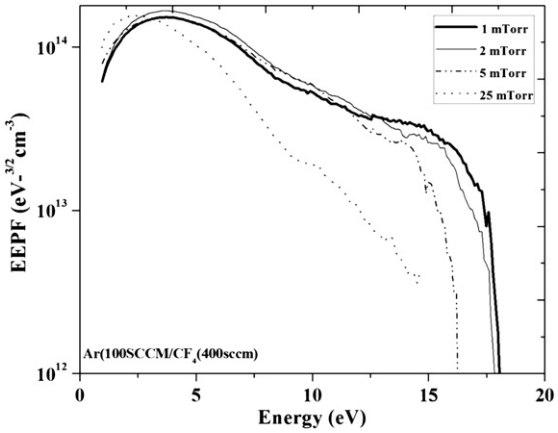

Fig. 6. EEPFs at the four chosen pressures of 1, 2, 5, and 25 mTorr. The rf powers have been kept fixed at 1000 W/1000 W ($P_{2MHz}/P_{13.56\ MHz}$) at the Ar/CF_4 gas flow ratios of 100 sccm/400 sccm.

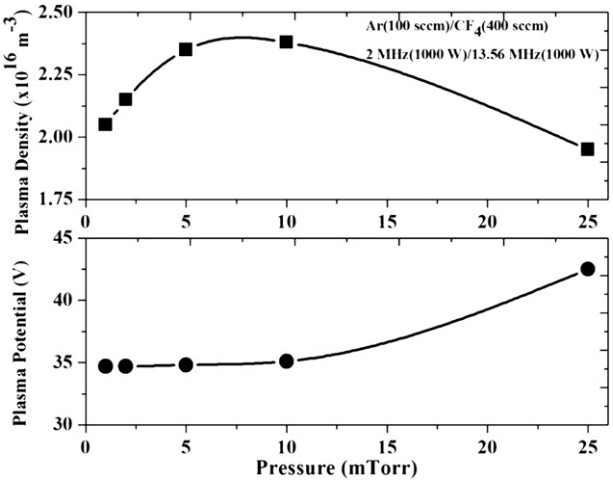

Fig. 8. Effect of pressure on the electron density and the plasma potential. The Ar/CF_4 gas flow ratio is 100 sccm/400 sccm. The rf powers have been kept fixed at 1000 W/1000 W ($P_{2MHz}/P_{13.56\ MHz}$).

that the higher the low frequency power (P_{2MHz}) content, the higher the density of higher energetic electrons. On the contrary, the higher the high frequency power ($P_{13.56MHz}$) content, the lower the population density of higher energy electrons. High energy electron population density increases with the increase of low frequency power (P_{2MHz}). It suggests that low frequency power (P_{2MHz}) is preferentially utilized to produce high energetic electrons. The measurements performed at all the three chosen total powers of 2250, 2000 and 1750 W, have the similar trend, as discussed earlier. Power ratio dependence of EEPFs shows similar behavior at all the chosen pressure (not shown here).

The basic plasma parameters, the plasma density n_e and the effective electron temperature Te were found from integrals of the EEPFs. The plasma potential has been estimated from maxima in doubly differentiated I–V probe characteristics. The pressure dependence on these discharge parameters (plasma density, plasma potential and electron temperature) is illustrated in Figs. 8 and 9. The rf powers have been kept fixed at 1000 W/1000 W ($P_{2MHz}/P_{13.56MHz}$). At low pressures (1 to 5 mTorr), plasma density linearly increases and electron temperature decreases (see Fig. 9) with pressure. The plasma potential is almost constant. However, a decrease in plasma density and increase in plasma temperature are observed at beyond 10 mTorr. It may attributed to increased electron heating at this pressure (25 mTorr). It decreases at pressure of 25 mTorr. The electron temperature linearly decreases at low pressure This observed decrease in plasma density at 25 mTorr is associated with increased plasma potential and electron temperature. The plasma potential is almost constant at low pressures (1–5 mTorr) and increases at 25 mTorr [24,25].

4. Conclusions

The pressure and gas ratio dependence on EEPFs and plasma parameters has been investigated in dual frequency large area inductively coupled plasma source. The plasma source comprises of two coils powered by 2 and 13.56 MHz separately. It has been observed that the EEPFs change from three temperature structure to Maxwellian type as pressure is increased from 1 to 25 mTorr.

It has also been observed that increasing pressure reduces energy spread of electron energy probability functions (EEPFs), due to increasing electron energy loss via collisions. The spread of EEPFs is 20 eV at 1 mTorr and it reduces to 13 eV at 25 mTorr. At a constant RF power, plasma density (n_e) increases linearly with pressure between 1 and 10 mTorr and then (>10 mTorr) decreases. The same trend has also been observed for electron temperature. It has also been found that increasing Ar gas proportion in Ar/CF_4 mixture significantly increases plasma density (n_e), however electron temperature and plasma potential have weak dependence on pressure.

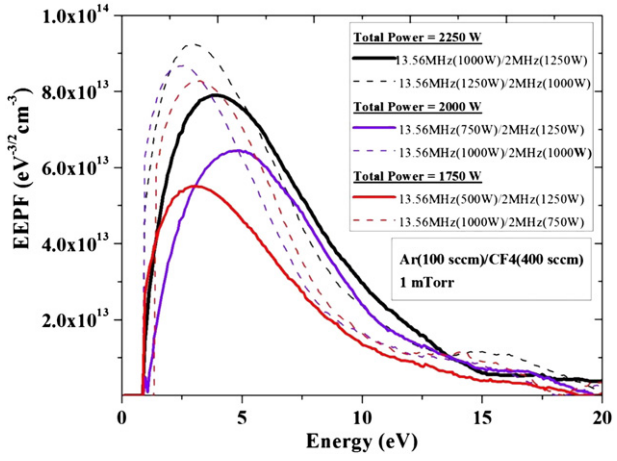

Fig. 7. EEPFs at the pressure of 1 mTorr. The total RF powers ($P_{2MHz} + P_{13.56\ MHz}$) have been kept fixed at 2250, 2000, and 1750 W. The Ar/CF_4 gas flow ratio is 100 sccm/400 sccm.

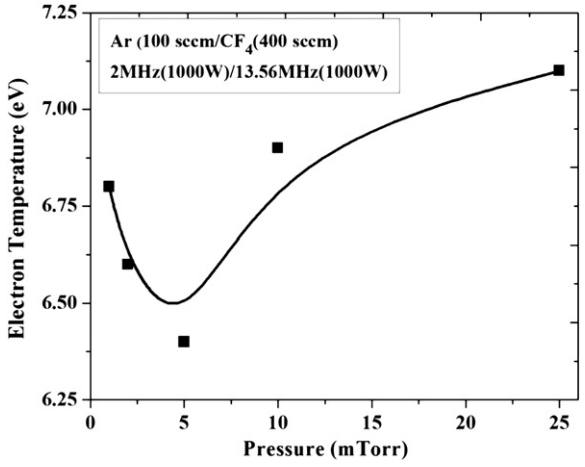

Fig. 9. Effect of pressure on the electron temperature. The Ar/CF_4 gas flow ratio is 100 sccm/400 sccm. The rf powers have been kept fixed at 1000 W/1000 W ($P_{2MHz}/P_{13.56\ MHz}$).

Acknowledgments

This work was supported by the Industrial Strategic technology development program (10041926, Development of high density plasma technologies for thin film deposition of nanoscale semiconductor and flexible display processing) funded by the Ministry of Knowledge Economy (MKE, Korea). This work was also supported by the Industrial strategic technology development program (KI002182, TFT backplane technology for next generation display) funded by the Ministry of Knowledge Economy (MKE, Korea).

This work was supported in part by the World Class University program of National Research Foundation of Korea (Grant No. R32-10124).

References

[1] C.Y. Chang, S.M. Sze, ULSI Technology, McGraw-Hill, New York, 1996. 329.
[2] J. Hopwood, Plasma Sources Sci. Technol. 1 (1992) 109.
[3] M. Kahoh, K. Suzuki, J. Tonotani, K. Aoki, M. Yamage, Jpn. J. Appl. Phys. 1 40 (2001) 5419.
[4] http://www.itrs.net.
[5] W.Z. Collision, T.O. Ni, M.S. Barnes, J. Vac. Sci. Technol. A 16 (1998) 100.
[6] S. Rauf, K. Bera, K. Collins, Plasma Sources Sci. Technol. 17 (2008) 035003.
[7] W. Tsai, G. Mueller, R. Lindquist, B. Frazier, V. Vahedi, J. Vac. Sci. Technol. B 14 (1996) 3276.
[8] K. Bera, S. Rauf, K. Ramaswamy, K. Collins, J. Appl. Phys. 106 (2009) 033301.
[9] T. Gans, J. Schulze, D. O'connell, U. Czarnetzki, R. Faulkner, A.R. Ellingboe, M.M. Turner, Appl. Phys. Lett. 89 (2006) 261502.
[10] M.A. Lieberman, J.P. Booth, P. Chabert, J.M. Rax, M.M. Turner, Plasma Sources Sci. Technol. 11 (2002) 283.
[11] G.A. Hebner, E.V. Barnat, P.A. Miller, A.M. Paterson, J.P. Holland, Plasma Sources Sci. Technol. 15 (2006) 879.
[12] P. Chabert, J. Phys. D. Appl. Phys. 40 (2007) R63.
[13] I. Lee, D.B. Graves, M.A. Lieberman, Plasma Sources Sci. Technol. 17 (2008) 015018.
[14] A. Mishra, K.N. Kim, T.H. Kim, G.Y. Yeom, Plasma Sources Sci. Technol. 21 (2012) 035018.
[15] A. Mishra, T.H. Kim, K.N. Kim, G.Y. Yeom, J. Phys. D. Appl. Phys. 45 (2012) 475201.
[16] A. Mishra, T.H. Kim, K.N. Kim, G.Y. Yeom, Plasma Sources Sci. Technol. 22 (2013) 015022.
[17] D. Barton, J.W. Bradley, D.A. Steele, R.D. Short, J. Phys. Chem. B 103 (21) (1999) 4423.
[18] M.A. Lieberman, A.J. Lichtenberg, Principle of Plasma Discharges and Material Processing, Wiley, New York, 1994.
[19] V.A. Godyak, R.B. Piejak, B.M. Alexandrovich, Plasma Sources Sci. Technol. 1 (1992) 36.
[20] F. Magnus, J.T. Gudmundsson, Rev. Sci. Instrum. 79 (2008) 073503.
[21] V.A. Godyak, R.B. Piejak, B.M. Alexandrovich, Plasma Sources Sci. Technol. 11 (2002) 525.
[22] J.P. Booth, G. Cunge, P. Chabert, N. Sadeshi, J. Appl. Phys. 85 (1999) 3097.
[23] H. Nishimura, W.M. Huo, M.A. Ali, Y.K. Kim, J. Chem. Phys. 110 (1999) 3811.
[24] M.V.V.S. Rao, M. Meyyappan, S.P. Sharma, J. Electrochem. Soc. 149 (10) (2002) C487.
[25] W. Liu, A. Zhu, X. Li, G. Zhao, W. Lu, Y. Xu, Y. Wang, Plasma Sci. Technol. 15 (2013) 9.